Dry Sliding Wear Behaviour of Plasma Sprayed Fly Ash Added Red Mud Coatings

Abstract: The present investigation aims at evaluating the effect of fly ash addition on sliding wear behaviour of pure red mud. Plasma sprayed coatings composed of red mud and varying percentage of fly ash were considered for the wear behavior study. Plasma spraying technique was involved at different levels of operating power (6, 9, 12 and 15 kW). Investigations of the coatings being divulged on the basis of some tribological properties like sliding wear behaviour, wear morphology, wear mechanism and frictional force. Experimental investigations also include the effect of varying percentage of fly ash on dry sliding wear behaviour of pure red mud. Fly ash with 10, 20 and 50 % by weight was mixed with red mud and allowed for the sliding wear test using pin on disc wear test machine. The wear test was performed for sliding distance of 94 to 942 m with track diameter of 100 mm and at sliding speed of 100 rpm (0.523 m/s); applying normal load of 10 N for a maximum duration of 30 minutes. The plots pertaining to the variation of wear rate and frictional force with that of sliding distance and time has been presented. Significant wear resistance being visible with the addition of fly ash due to increase in bond strength and dense film at interface.

Key words: Red mud; Fly ash; Plasma Coating; Sliding wear; Wear morphology; Frictional force; wear mechanism.

1. INTRODUCTION:

Coating technologies have already gained the promising momentum for the creation of emerging materials in the last few decades. Coatings with some advanced wear properties put a signature of claiming for the better use in tribological applications. Plasma spray is one of the most widely used techniques involved in surface modification by augmentation of wear resistance, which may affirm the great versatility and its application to a wide spectrum of materials. The coatings with considerable amount of hardness can protect against variety of wear mediums including abrasive, adhesive and corrosive. Basically, wear resistive coatings are fabricated by considering some common conventional materials like nickel, iron, cobalt and molybdenum based alloys, carbides of ceramic and tungsten [1-2]. Extensive

33 investigations pertaining to the erosion wear behavior of plasma sprayed ceramic coatings by

34 using Taguchi Technique being reported by some experimenters [3]. The tribological

35 properties of traditional manganese phosphate coatings and hBN composite coatings

36 composed of nano hexagonal boron nitride (hBN) in layered manganese phosphate crystals on

37 AISI 1040 steel were being divulged in some literatures [4].

38 In retrospection, literatures made available regarding the wear behaviour of WC with 12% Co

39 coatings produced by Air Plasma Spraying method at different standoff distances [5].

40 Examinations on the basis of the wear behaviour of Mo and Mo+NiCrBSi thermally sprayed

41 coatings being performed for the application as next generation ring face coatings [6]. Almost

42 all plasma sprayed ceramic coatings portrayed favorable tribological performance in linear

43 contact at high temperatures: high anti-wear resistance and easy to be lubricated owing to the

44 oil storage of pores in coatings [7-9]. But needful to say, plasma sprayed ceramic coatings

45 exhibit some failure mechanisms during sliding such as plastic deformation, brittle fracture

46 and polish effects [10], which in turn demands a few additives, which could reduce the

47 friction and wear of plasma sprayed ceramic coatings [11].

48 Several factors may influence the tribological behaviour of a coated surface ramified as: the

49 geometry of the contact including macro geometry and topography of the surfaces; the

50 material characteristics; basic mechanical properties as well the microstructure and finally the

51 operating parameters controlling the coating deposition [12].

52 Red mud as an industrial waste material is considered to be the material of choice for coating

53 applications. It is behooved to mention here that, red mud in present decade should be

54 considered as an alternative wealth for replacing some conventional expensive coating

55 materials. Utilization of red mud and its implications made available in literature [13] in great

56 details. Few results on the basis of wear behavior of red mud were being reported by some

57 researchers. In addition to above, morphology and solid particle erosion wear behaviour of red

58 mud and fly ash composite were being available in literature [14]. Characteristics of plasma

59 sprayed pure red mud coatings were being reported [15]. Red mud as filling material is also

60 found to be the wear enhancing agent for metals [16]. Data pertaining to the sliding wear

61 behavior of fly ash based red mud composite coatings are not abundant and need to be

62 addressed. The present investigation is an attempt in a direction to evaluate the wear behavior

63 of varying percentage of fly ash with pure red mud coating at different operating power

64 subjected to normal laboratory conditions. This articulated paper may pave the path for

65 furthering the study to throw some further light on fly ash based red mud coatings.

66

2. MATERIALS AND METHODS OF EXPERIMENTATION

2.1 Preparation of coating powder

The present experimental work included the preparation of coating powder considering the raw materials as red mud and fly ash powders. The powder mixture concomitants of red mud and different percentage of fly ash was being prepared and mixed using V-shaped drum mixer. In addition, pure red mud powder was also considered as coating material for the sake of comparison on the basis of percentage of fly ash addition. Coating of the various combinations of mixed powders was conducted on one side cross section of the mild steel substrate. Data pertaining to Table 1 contains the different combinations of the mixtures chosen for plasma spraying.

Table. 1 Powders used for coating deposition.

Sl.No.	Coating Material	Mixture Composition (By weight %)
1	Red Mud (RM)	100
2	Red Mud + Fly Ash (FA)	90 + 10
3	Red Mud + Fly Ash	80 + 20
4	Red Mud + Fly Ash	50 + 50

Red mud, as the primary raw material was collected in powder form from National Aluminium Company (NALCO) located at Damonjodi in the state of odisha, India. The as-received powder was sieved to obtain particles in the required size range of 80-100 μm. Raw fly ash was collected from the captive power plant of Rourkela steel plant, India and allowed for sieving to maintain same size range as that of fly powder. Powders having three different weight ratios of red mud and fly ash (Table 1) were extensively prepared by mixing thoroughly.

2.2 Preparation of substrates

Commercially available mild steel rod was mooted as source for substrate preparation. The rod was cut to some number of pieces having one particular dimension (l = 40 mm and Ø= 12 mm) each. The specimens were grit blasted from one side cross section (initial roughness 0.03 mm) at a pressure of 3 kg/cm^2 using alumina grits of grit size 60. The stand-off distance in the shot blasting was kept between 120-150 mm. Then the average roughness of the substrate was reported to be 6.8 μm. The grit blasted specimens were allowed for plasma spraying after cleaning in an ultrasonic cleaning unit.

2.3 Plasma spraying

The spraying process was performed at the Laser and Plasma technology division of Bhaba Atomic Research Centre, Mumbai, India by adopting conventional atmospheric plasma spraying (APS) set up. The plasma input power was varied from 6 to 15 kW by controlling

98   the gas flow rate, voltage and arc current. The powder feed rate was maintained to be constant
99   at 10 gm/min by using a turntable type volumetric powder feeder. Plasma generation
100 demanded the suitability by purging Argon as primary and Nitrogen as secondary gas agent.
101 The mixture of powders were being deposited at spraying angle of 90° by maintaining the
102 powder feeding as external to the gun. The properties of the coating are merely depends upon
103 the parameters of spraying process. The operating parameters maintained during coating
104 deposition process are being tabulated in Table.2.

105 **Table 2** Operating parameters during coating deposition

Operating Parameters	Values
Plasma Arc Current (Ampere)	200,225,250,300
Arc Voltage (Volt)	30,40,48,50
Torch Input Power (kW)	6,9,12,15
Plasma Gas(Argon), (litre/min)	20
Secondary Gas (Nitrogen), (litre/min)	2
Career Gas(Argon) Flow rate (litre/min)	7
Powder Feed Rate (gm/min)	10
Torch to base distance (mm)	110
Arc Length Range (mm)	2,3,6,8,11

106 *2.4 Pin on disc Wear Testing*

107 The above experiment was being conducted in the pin on disc type friction and wear
108 monitor (DUCOM; TR-20-M100) with data acquisition system. The concerned machine was
109 used to evaluate the wear behavior of the coatings against hardened ground steel disc (En-32)
110 having hardness of 65 HRC and surface roughness (Ra) 0.5 µm. The versatility of the
111 equipment lies behind the design to study the wear behaviour under un-lubricated sliding
112 condition, which occurs between a stationary pin and a rotating disc.
113 The disc of the machine rotates with the help of a D.C. motor having speed range of 0-200
114 rpm with wear track diameter 0-160 mm; which can yield sliding speed of 0-10 m/s. Load is
115 to be applied on pin (specimen) by dead weight through pulley string arrangement. The
116 system has a maximum loading capacity of 500 N. For the present experimentation, pin
117 specimen was kept stationary perpendicular to disc, while the circular disc was rotated as
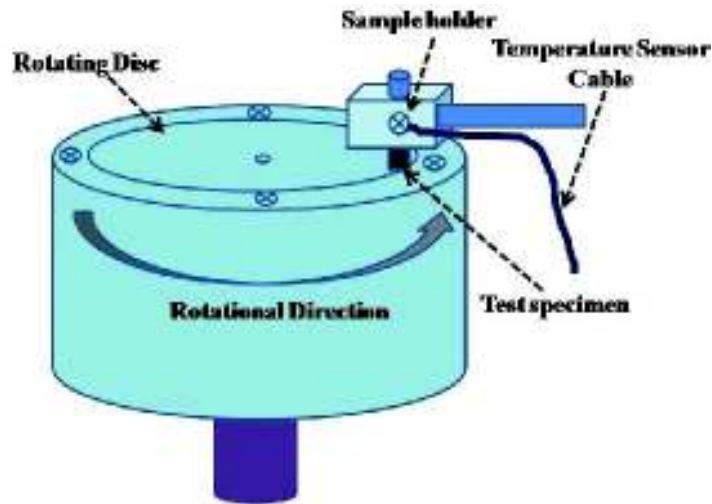118 shown in Figure 1.
119
120

121
122

Figure.1 Schematic Representation of Pin on Disc Apparatus

3. **RESULTS AND DISCUSSION**

3.1 Scanning electron microscopy and Compositional analysis

The characterization of red mud powder involved taking microstructures by the help of Scanning electron microscope (JEOL; JSM-6480 LV). The micro structural images captured by SEM (Scanning electron microscope) and EDS (energy dispersive spectroscopy) analysis of pure red mud powder were being illustrated in Figure 2. EDS experiment was performed by the help of SEM of above specification with the required attached module. Data presented in Table 3 indicates the weight as well the atomic percentage of elements comprising pure red mud powder. The EDS analysis of red mud revealed the signature of some elements like Fe, Al, Si, O and some other minor constituents. The prominent constituent of red mud was found to be iron with its oxides. The EDS analysis of red mud with 20 % fly ash coatings prepared at 9 kW of operating power was shown in Figure 3. In addition, the analogous elemental analysis relating Figure-3 was reported in Table.4, indicating the increase in silica and iron constituents in the composite coating.
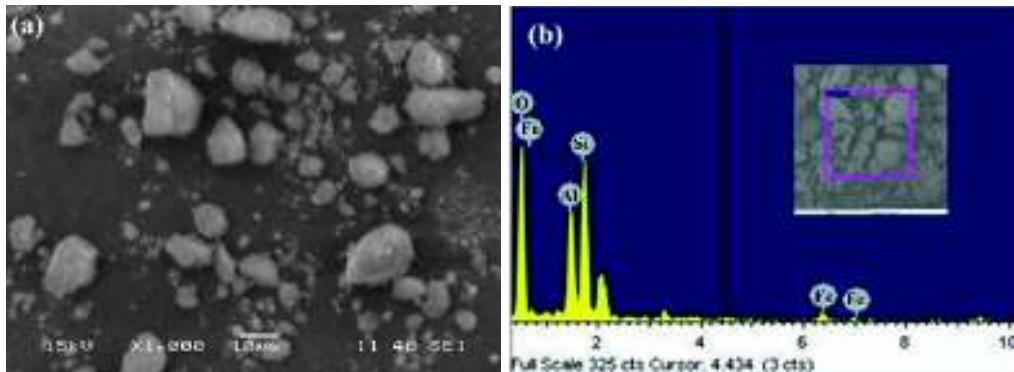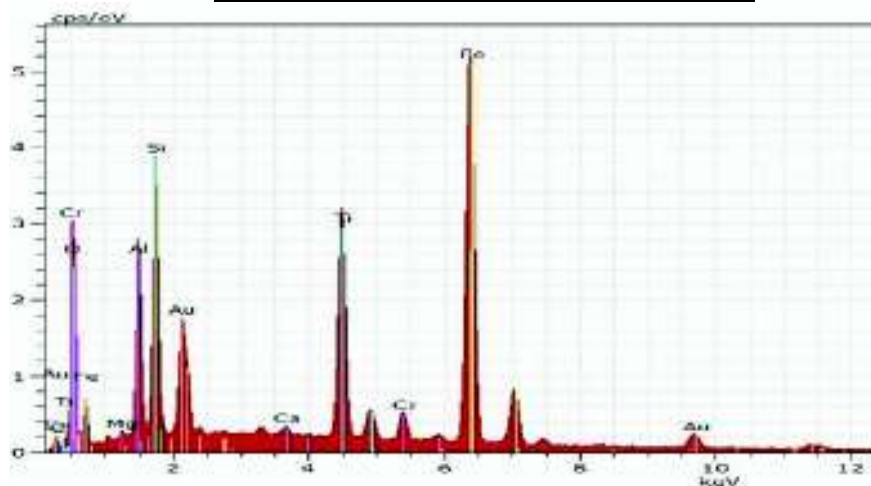

138

139   Figure 2. (a) SEM and (b) EDS analysis of Red Mud
140

141

142

Table 3. Elemental analysis of Red mud

Element	Weight%	Atomic%
C K	24.59	33.29
O K	23.65	24.54
Al K	7.41	4.47
Si K	12.21	7.07
Fe K	32.14	30.62
Totals	100.00	

143

144

Figure 3. EDS analysis of RM+20 % FA Composite coating at 9 kW

145

146

147

148

149

Table 4. Elemental analysis of RM+20 % FA Composite coated at 9 kW

Element	Weight %	Atomic %
Fe K	36.13	25.90
O K	21.74	42.61
Ti K	14.02	9.18
Si K	17.10	7.93
Al K	6.59	7.66
Cr K	2.14	1.29
C K	1.99	5.20
Ca K	0.29	0.22
Au K	0.00	0.00
Mg K	0.00	0.00

Totals	100 %	100

3.2 Coating porosity

Image analysis technique was adopted for the measurement of porosity of coating materials. The polished surfaces of various coatings were kept under a microscope (Neomate) equipped with a charge coupled-device (CCD) camera (JVC, TK 870E). Volume of interest (VOIS) image analysis software paid an important role for the determination of porosity. The software can measure accurately the total area captured by the objective of the microscope. Hence the total area and the area covered by the pores are separately measured to report porosity. The "VOIS image analysis software" used in this analysis is being licensed by the authors. The porosity data of three different coating powders are being tabulated in Table.5. A cross sectional view of red mud coating prepared at 9 kW of operating power was captured by the help of field emission scanning electron microscope (FESEM; Nova Nano SEM-450), as shown in Figure 4.
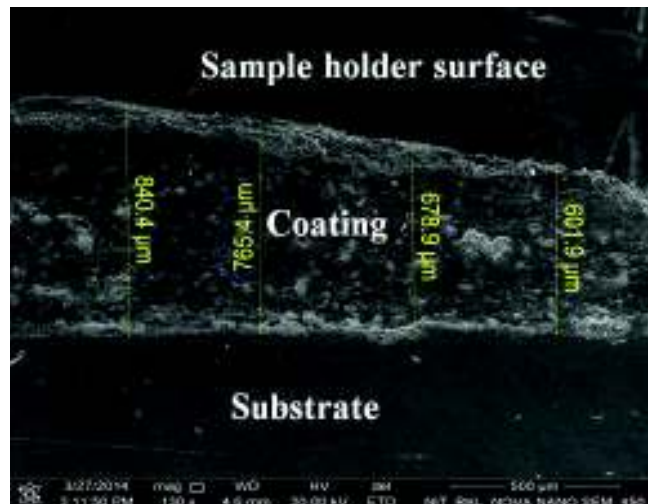

Figure 4. FESEM image of coating Cross section of pure red mud at 9 kW

Table 5. Coating Porosity for different coating type.

Coating Material	Plasma Torch Input Power(kW)	Porosity (%)
Red Mud	6	12.89
	9	12.02
	12	11.87
	15	13.02
90 % Red Mud	6	11.52

+	9	11.12
10 % Fly Ash	12	10.90
	15	12.98
80 % Red Mud	6	10.89
+	9	10.54
20 % Fly Ash	12	10.17
	15	11.78

168   Approximately 8-13% porosity range was observed (Table-3) for all three coating
169   materials. Porosity amount was found to be ameliorated in case of all coating compositions
170   prepared at lower (6 kW) and at higher (15 kW) power levels. At 6 kW operating power level,
171   there is poor melting of particles subjected to relatively low plasma gas temperature
172   exhibiting non-uniform mixing of molten particles; which in turn causes reasonably porous
173   coating layer. On the other hand, at highest operating power level (15 kW) the high plasma
174   gas temperature caused faster deposition of molten particles by creating thickened coating
175   layer with less hardness and high porosity.

176   Porosity level was found to be higher in case of pure red mud compared to the composite
177   coatings pertaining to the mixture of fly ash and red mud. About 3-10% porosity level was
178   reported for the coatings prepared by conventional plasma spraying [17], which in turn
179   authenticates the porosity results as obtained in the present investigation.

180   *3.3 Coating Hardness*

181   The polished section of the coatings put under optical microscope for the microscopic
182   observations, which revealed the presence of three distinguishable different phases namely
183   dull, white and spotted. The three different distinct phases are allowed for micro indenting to
184   record Micro hardness data with the help of Leitz Micro-Hardness Tester using 50 Pa
185   (0.493 N) on all samples. The results are summarized in Table.6. The three structurally
186   different phases of red mud coatings bear three different ranges of hardness values varying
187   from 488 to 588 HV. Hardness values were found to be enhanced for the composite coatings
188   belonging mixture of red mud and fly ash. This result is attributed due to the increased content
189   of alumina and silica in the composition of feed material forming alumino-silicate (mullite
190   phase) during spray deposition [18].
191

192   **Table 6.** Coating Hardness for different operating power level

Coating Material	Plasma Torch Input Power (kW)	Micro Hardness (HV)		
		Dull	White	Spotted
100% Red Mud	6	540	488	496
	9	532	498	511
	12	586	513	508
	15	555	502	510
90% Red Mud	6	638	632	628
+	9	648	642	636

10 % Fly Ash	12	660	638	628
	15	651	640	632
80 % Red Mud	6	658	649	642
+	9	669	658	649
20 % Fly Ash	12	699	689	652
	15	681	681	650
50 % Red Mud	6	696	679	658
+	9	682	633	672
50 % Fly Ash	12	726	712	660
	15	719	679	668

193   *3.4 Wear test study*

194   Prior to the starting of the wear testing experiment, the pin and the disc surface of the
195   concerned equipment were polished perfectly with emery papers for better ensuring of smooth
196   contact with the coating samples. Hereafter the surface roughness lessens by a magnitude of
197   0.1 µm. The wear tests were carried out as per ASTM G- 99 standard for maximum time
198   period of 30 minutes under un-lubricated condition in a normal laboratory ambience having
199   relative humidity of 40-55% and the temperature range of 20-25°C. The weight of the
200   specimens before and after the wear experiment were being recorded by using electronic
201   weighing machine having accuracy up to second decimal limit (0.01 mg) for monitoring the
202   mass loss occurrence in the coating samples. Specimens were taken care of in particular for
203   cleaning with woolen cloth to avoid entrapment of wear debris and to maintain uniformity in
204   each set of experiments. The test pieces are cleaned with tetrachloroethylene solution before
205   and after each test. Wear rate was estimated by measuring the mass loss (Δm) in the specimen
206   after each test. Wear rate relating to mass loss and the sliding distance (L) was formulated
207   below in equation (1).
208

$$W_r = \frac{\Delta m}{L}$$ (1)

209   where W_r = Wear rate in N/m;
210   Δm = Mass Loss in Newton (N);
211   L = Sliding distance in meter (m).
212   The frictional force (F) was measured directly from the apparatus in 'kg' at each time
213   interval.
214   The wear experiment was chalked out at normal atmospheric temperature under a constant
215   normal force of 10 N and a fixed speed of 100 rpm. The track diameter of the equipment was
216   kept at 100 mm. The maximum duration of sliding was 30 minutes comprising of 10 intervals
217   with each having 3 minutes of time gap. Each sample specimen was allowed for sliding for
218   distinct time interval.
219   Initially, the experiment was performed with red mud coated samples and then continued
220   for fly ash based red mud coating composites. Figure 5 illustrates the variation of wear rates
221   with sliding distance for different operating power levels.

The wear results for pure red mud coating operated at 6 kW of operating power being visible in Figure 5 (a) disclosing the variation of wear rate with minimum value of 0.11 N/m to maximum value of 0.45 N/m. The wear rate value was found to be increased from 0.11 to 0.13 N/m for first 6 minutes of sliding. The wear rate plot affirmed a plateau just after a drastic increasing trend from 6 to 12 minutes of duration. The plateau in wear rate value may be attributed due to the variation of coating layer property. This is one fact indicating the more hardness of denser surface of top layer than that of bulk layer. The change of coating property just after 6 minutes of sliding may be due to the coating property variations bearing less hardness of bulk layer.

The wear rate was reduced for fly ash based (10%, 20% and 50%) composite coatings, as being illustrated in Figure 5. This indicative trend of wear rate for fly ash composite coatings are quite similar to that of pure red mud coating. Substantial slow increase in wear rate for the composite coatings was being visible followed by a drastic gain. Henceforth, the wear rate was constant for all composite coating type. The plots pertaining to Figure 6 represent the variation of wear rates of each coating type with that of sliding distance for different operating power level.

The effect of operating power level on wear rate is quite interesting. The wear rate is resulted attributing to the porosity and hardness. The wear rate was found to be enhanced up to 12 kW and departing result for 15 kW. The wear rate for 15 kW was found to be lied between 9 and 12 kW. This might be due to the improper particle to particle bonding and poor stacking to the substrate, which in turn lowered the hardness as well as density due to poor interfacial bond strength. Figure 7 shows the trends of wear rate for all coating materials against operating power level for a particular sliding time (15 minutes).

An experimental study on coating thickness for fly ash and red mud composite with operating power is reported [18]. An increase in coating thickness with increase in input power to the plasma torch; up to about 12 kW is observed and then with further higher input power no improvement in coating thickness is recorded.
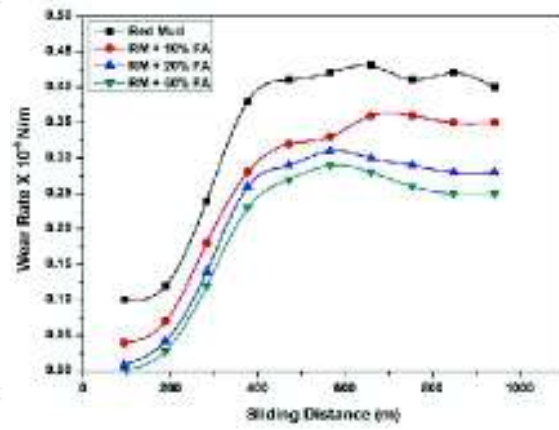
The frictional force (F) in kg was measured directly from wear apparatus deputed for the present investigation. The graphical representation concerning the variation of frictional forces with that of sliding time is focused on Figure 8, which includes the picture for all coating materials and also for operating power levels considered. As per the observations, maximum frictional force is evidenced for pure red mud coating and being decreased with the addition of fly ash, akin to the results as being occurred for wear rate. An increase in frictional force up to a maximum value of 0.63 kg for pure red mud coating at 12 minute sliding time is being observed followed by a fluctuating wavy response up to 21 minutes then a constant magnitude up to 30 minute of sliding.

Figure 9 shows the comparative study relating frictional forces for the coating composites with 10% fly ash. The frictional force is found to be maximum at 6 kW and be minimum at 12 kW operating power. At 15 kW of operating power, the frictional force was reported to be in range of values whatever lies for the power levels in between 9 to 12 kW. These results are in accordance with the findings as being observed for wear rates.
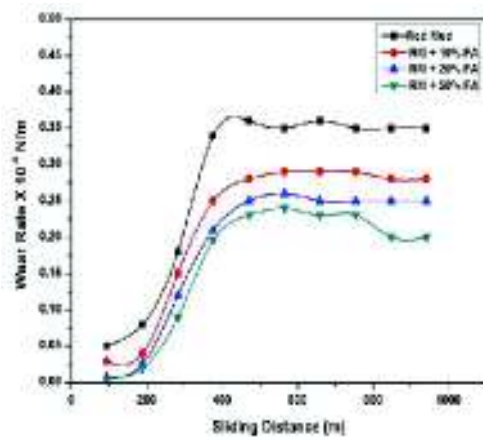
264
265   Wear morphology for selected coating samples were being highlighted in some images
266 captured by FESEM. Figure 10 represents the wear morphological images for red mud with
267 10% fly ash coating (prepared at 6 kW operating power) allowed for sliding for the time
268 intervals of 3, 6, 12 and 15 minutes. Owing to continuous sliding of counter surfaces, wear
269 debris formed which interlocks within sliding interface attributing pitting and eventually crack
270 formation. Wear scars, debris formed and cracked sections are being clearly visible in Figure
271 10 (b) and Fig 10 (d) assigning to a fatigue failure in the real sense on the worn surface.
272 Figure 11 shows the worn surfaces for 50 % fly ash based red mud coatings (prepared at 12
273 kW of operating power level) for the sliding intervals 3, 6, 12, 15, 27 and 30 minutes. The
274 wear morphology changes with increase in the sliding distance impacting change in surface
275 roughness leading to the interruption of its contact mechanism. The change in wear
276 characteristics may be attributed due to the variation of hardness of coating inter-layers with
277 respect to the change in sliding distance. At incipient, a slow increase in wear rate is observed
278 and then attains a rapid increment, the 'break in' situation, after traversing of certain sliding
279 distance. The further increase in sliding distance cannot change the contact area; causing a
280 relatively steady wear rate. Hence, it can be concluded that the wear takes place by the
281 phenomenon of adhesion and abrasive mechanism due to development of shear stresses in
282 between the hard asperities of the two surfaces in contact. After the "break in" phase, the
283 trend of wear rate remains almost constant for coatings deposited at all power levels. The
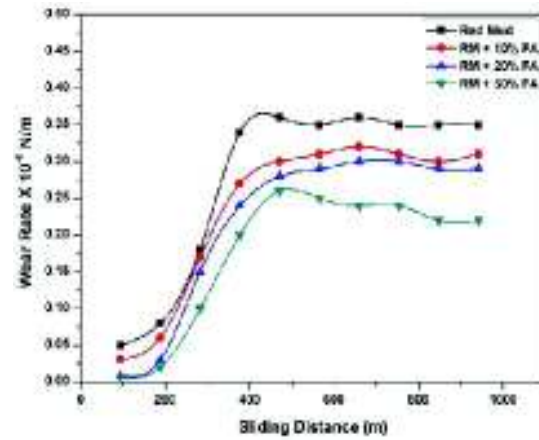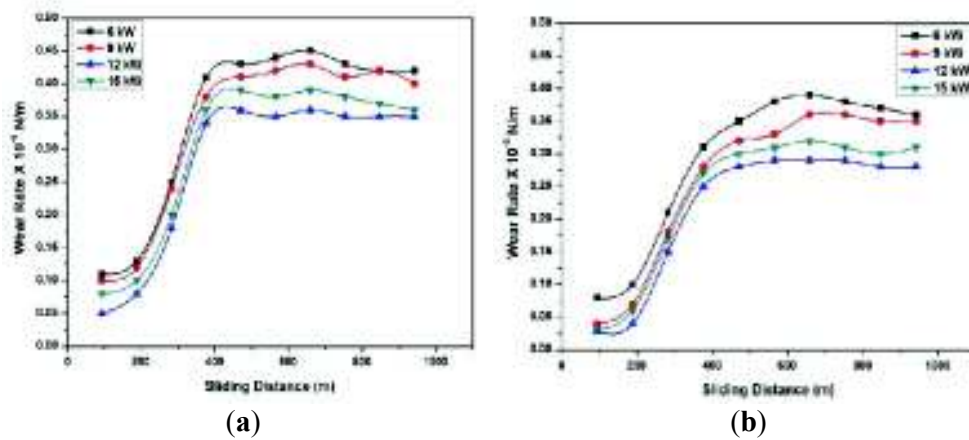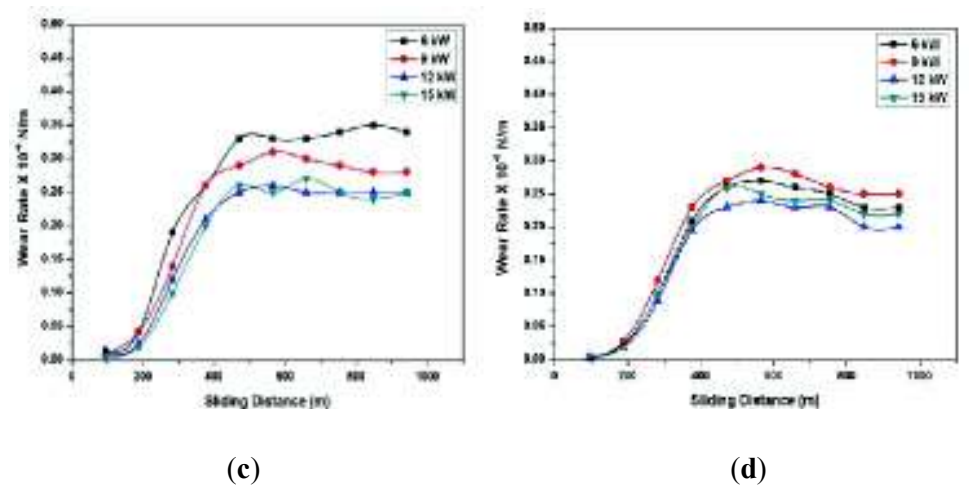284 duration of this stage extends till the end of the test.

285
286
287
288
289
290
291
292
293
294
295
296
297

298

(**a**)
(**b**)

299

300
(**c**)
(**d**)
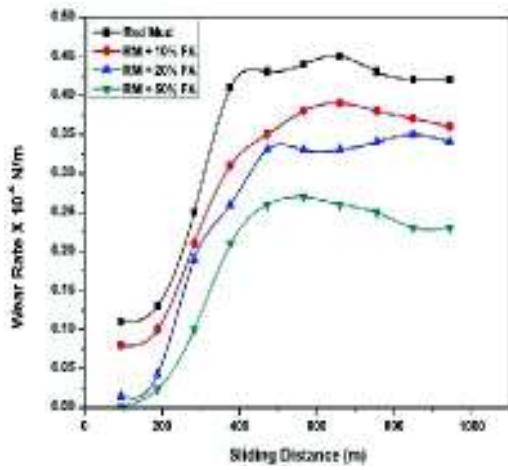
301　Figure.5. Wear Rates obtained for different coating type with sliding distance. (a) 6 kW, (b) 9
302　　　　　　　　　　　　　　　　KW, (c) 12 kW, (d) 15 kW.
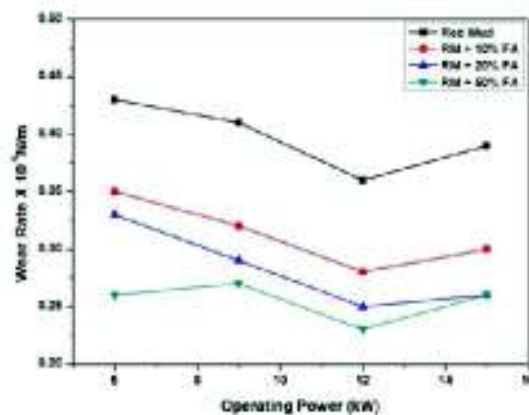
303
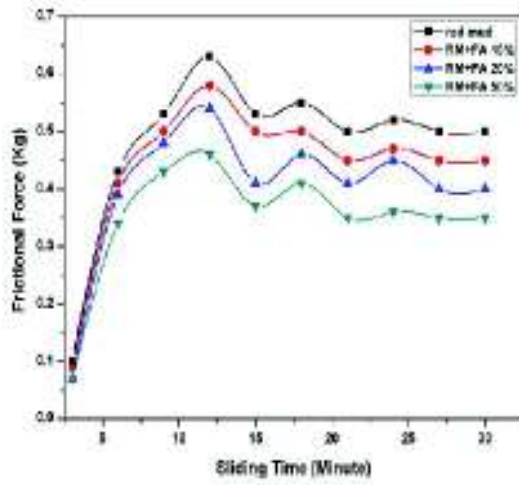

(**a**)

(**b**)

304

(**c**)

(**d**)

305

306 Figure 6. Wear rate comparison for different operating power level. (a) Red Mud,
307 (b) Red Mud +10 % Fly Ash, (c) Red Mud+20% Fly Ash, (d) Red Mud+50% Fly
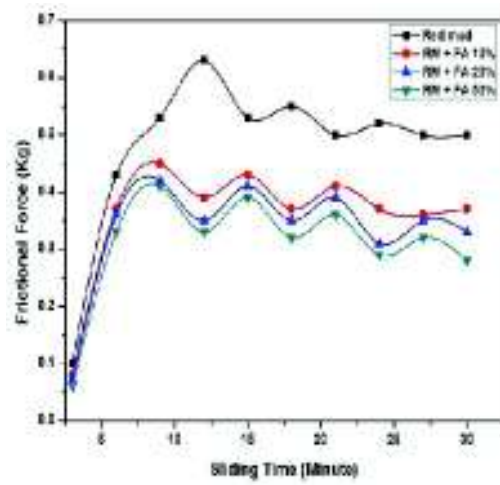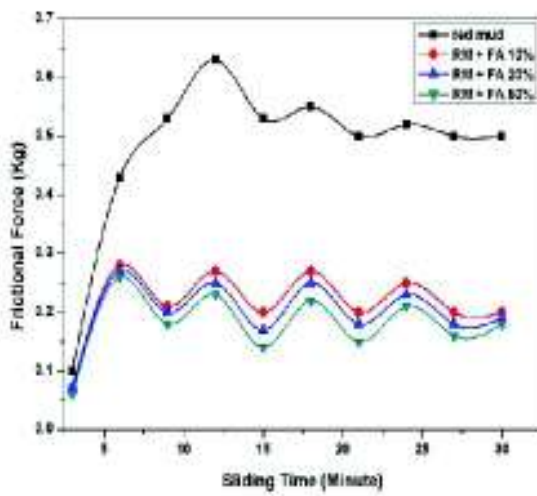308 Ash.

309

310 Figure 7. Variation of wear rate with operating power level at sliding time of 15
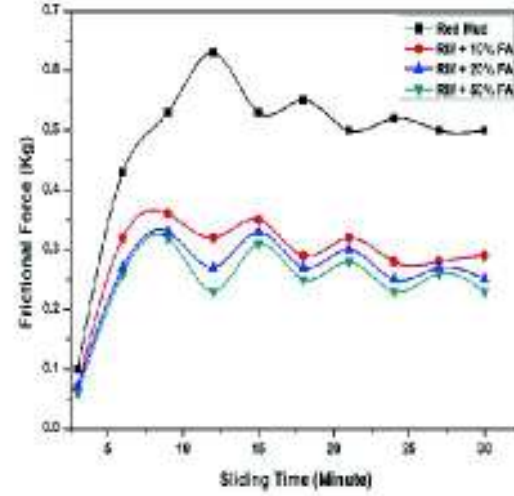311 minute.

13

312

313

(a)   (b)

315

317   (c)   (d)

318

319   Figure.8. Frictional forces against sliding time for all coating type. (a) 6 kW, (b) 9 kW,
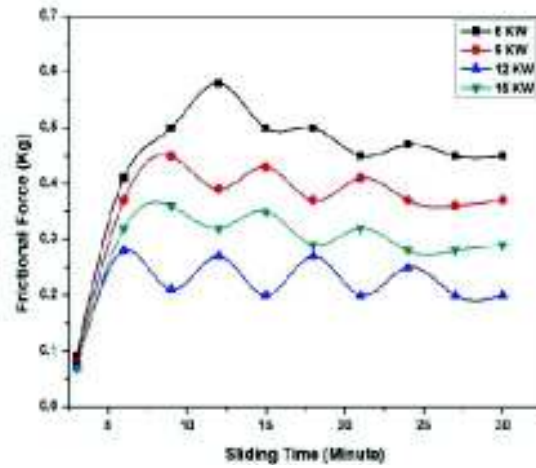
320   (c) 12 kW, (d) 15 kW.

321

322   Figure.9. Comparison of frictional force values for 10 % fly ash coating.
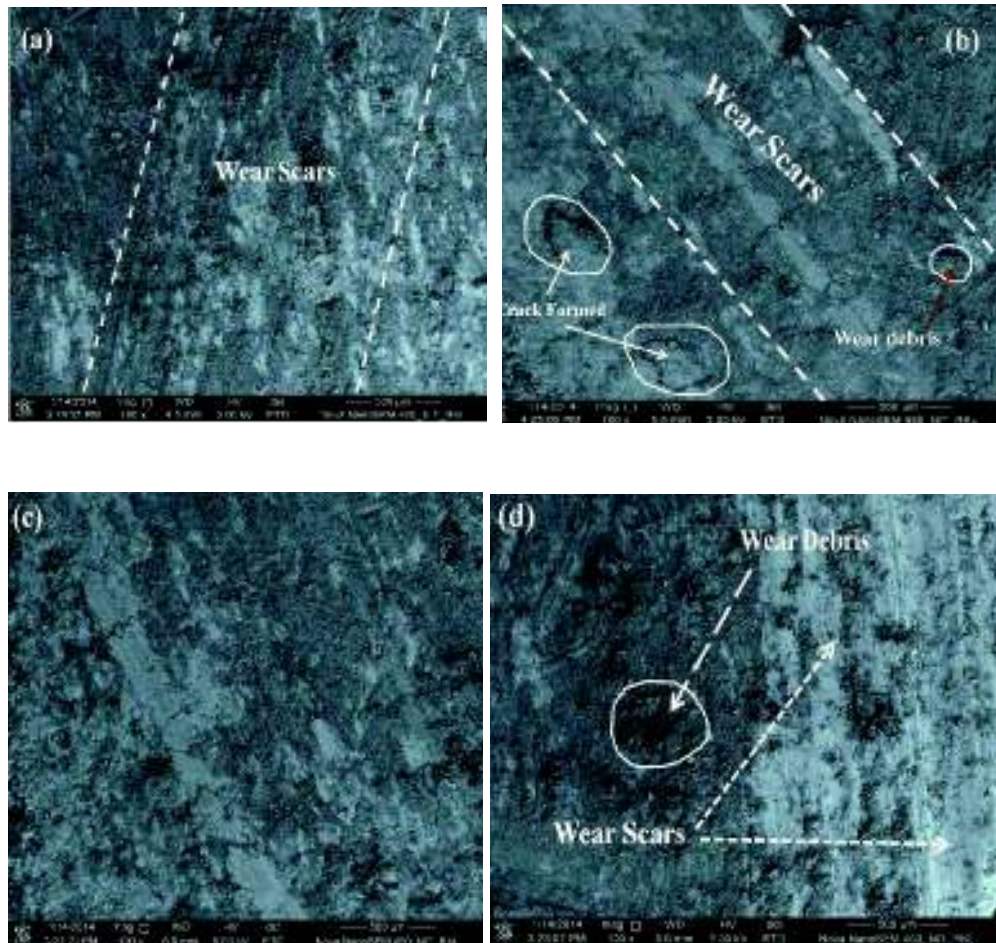

323
324

325

326   Figure.10. Worn Surfaces for Red Mud + 10 % Fly ash coatings for 6kW
327   Operating Power Level.; (a) 3, (b) 6, (c) 12 and (d) 15 minutes time interval.
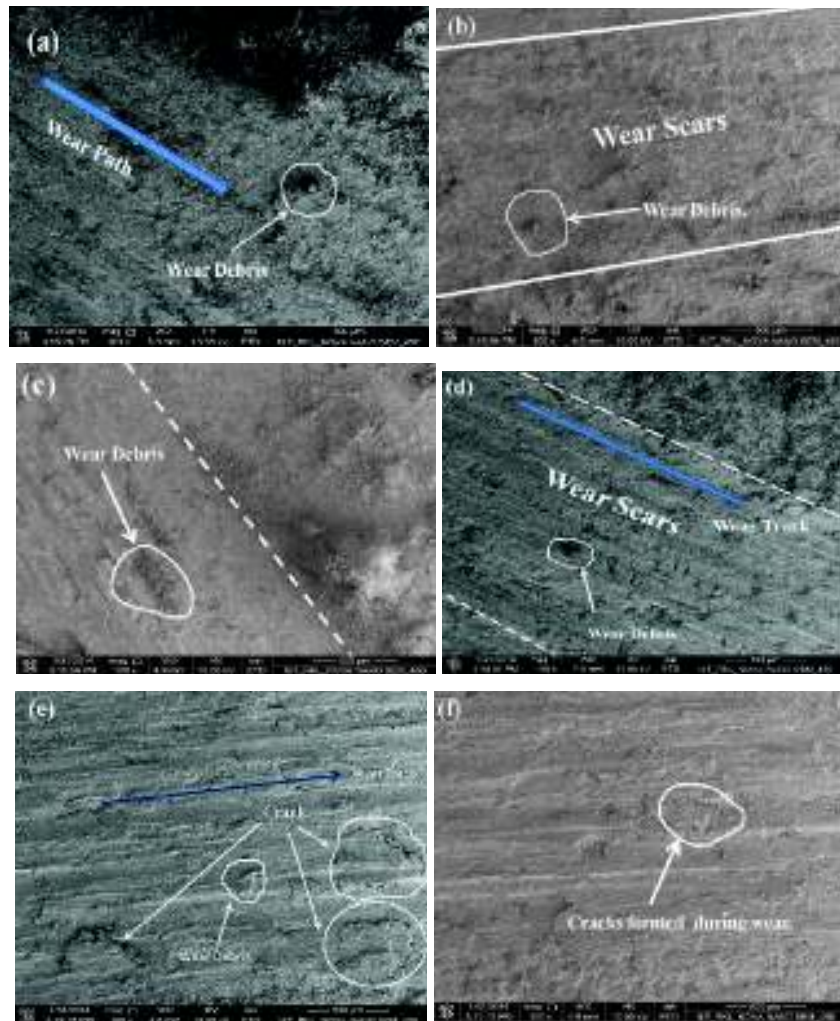
Figure.11. Worn Surfaces for Red Mud + 50 % Fly ash coatings for 12 kW Operating Power Level.; (a) 3, (b) 6, (c) 12 ,(d)15, (e) 27 and (f) 30 minutes time intervals.

4. CONCLUSION

The present experimental investigations are being winded up with some salient concluding remarks. Red mud, the waste generated from alumina plants is eminently coat able on metal substrates by employing thermal plasma spraying technique with excellent wear resistance. Addition of fly ash with red mud reduces the wear rate by enhancing the coating mechanism and hardness. But the optimum percentages of fly ash required for better coating material still impact a question mark for the researchers. It is observed that for the early stage the wear rate increases slowly and then drastically improved with sliding distance for all coating type and finally becomes stagnant. Operating power level proved to be the remarkable variable for coating property; which enhances the coating resistance, but afterwards with reaching an optimum value indicating some other dominating parameters. The present work leaves with some wide spectrum of scopes for future investigators to explore many other aspects of red

mud coatings. Thermal stability of these coatings may be evaluated for better claiming in high temperature applications. Corrosive wear behavior under different operating conditions may be investigated to identify suitable application areas. Post heat treatment of these coatings may also be implemented further for furthering the study regarding the improvement in coating quality and properties.

CONFLICT OF INTEREST

The authors declare no conflict of interest exist for publishing this paper.

References

1. Kushner, B.A and Novinski, E.R. "Thermal spray coating," *ASM Hand book*, **18** (829-833).1992.
2. Crook, P; "Friction and wear of Hard facing Alloy," *ASM Hand book*, **18** (758-765), 1992.
3. Mishra,S.C., Das, S.,Satapathy, Alok., Ananthapadmanabhan P.V., and Sreekumar, K.P, "Erosion Wear Analysis of Plasma Sprayed Ceramic Coating Using the Taguchi Technique," *Tribology Transactions*, 2009, vol.52, no**.**3, pp. 401-404.
4. Ay, N., Nuri Çelik,O., and Göncü, Y, "Wear Characteristics of Traditional Manganese Phosphate and Composite hBN Coatings," *Tribology Transactions*, 2013, vol.56, no.6, pp 1109-1118.
5. Afzal, M., Ajmal, M., and Khan, A. N, "Wear Behavior of WC-12% Co Coatings Produced by Air Plasma Spraying at Different Standoff Distances," *Tribology Transactions,* 2014*,* vol.57,no.1, pp 94-103.
6. Waynea,S.F., Sampath., S and Anand, V, "Wear Mechanisms in Thermally Sprayed Mo-Based Coatings", *Tribology Transactions*, 1994, vol.**37**,no.3 pp 636-640.
7. Wang, Y., Jin,Y and Wen,S, "The analysis of the friction and wear mechanisms of plasma-sprayed coatings at 450°C," *Wear*, 1998, vol.**128** , pp. 265–276.
8. Wang, Y., Jin,Y and Wen,S, "The analysis of the chemical structure and properties of ceramic surface films in friction using SEM, AES and Micro-region X-ray diffraction," *Wear*, 1998, vol.**128**, pp. 277–290.
9. Wang, Y., Jin,Y and Wen,S, "The inspection of sliding surface and subsurface of plasma-sprayed using scanning acoustic microscopy," *Wear*, 1998, vol.**134**, pp. 399–411.
10. Vijande-Diaz,R., Belzunce,J., Fernandez,E., Rincon, A and Pérez,M.C ,Wear and microstructure in fine ceramic coatings, *Wear*, 1991,vol.**148**, pp. 233–331.
11. Wei,J and Xue,Q, "Effects of additives on friction and wear behaviour of Cr_2O_3 coatings," *Wear*, 1993, vol.**160** , pp. 61–65.
12. Homberg, K., Mathews,A and Ronkainen, H, "Coatings Tribology-Contact mechanisms and surface design," *Tribology International*,1998, **31**(1-3), pp 107-120.

384 13. Sutar,H., Mishra,S.C., Sahoo,S.K., chakraverty,A.P. and Maharana,H.S,"Progress of
385   Red Mud Utilization: An Overview," *American Chemical Science Journal,* 2014 *,*
386   vol.4,no.3, pp 255-279.

387 14. Sutar, H., Mishra, S.C., Sahoo, S.K., Satapathy, A and Kumar, V., "Morphology and
388   solid particle erosion wear behaviour of red mud composite coatings." *Natural*
389   *Science*, 2012, vol.4, no.11, 832-838.

390 15. Satapathy,A., Sutar,H., Mishra,S.C and Sahoo,S.K, "Characterization of Plasma
391   Sprayed Pure Red Mud Coatings: An Analysis," *American Chemical Science Journal*,
392   2013, vol.3 no.2, pp 151-163.

393 16. Prasad,N., Sutar,H., Mishra,S.C., Sahoo,S.K and Acharya,S.K, "Dry sliding wear
394   behavior of aluminium matrix composite using red mud an industrial waste,"
395   *International Research Journal of pure and applied chemistry*, 2013, vol.3,no.1, pp
396   59-74.

397 17. Pawlowski, L,"The Science and Engineering of Thermal Spray Coatings," John Wiley
398   & Sons, New York , pp. 218, 1995.

399 18. Satapathy, A., "Thermal Spray Coating of Red mud on Metals" *PhD Thesis*, National
400   Institute of Technology, Rourkela, Odisha, India, 2005.

401

402